RSC Advances

PAPER

View Article Online
View Journal | View Issue

Cite this: *RSC Adv.*, 2014, **4**, 48465

A sandwich-like electrochemiluminescent biosensor for the detection of concanavalin A based on a C_{60}–reduced graphene oxide nanocomposite and glucose oxidase functionalized hollow gold nanospheres

Juanjuan Zhang, Yuan Ruo, Shihong Chen,* Xia Zhong and Xiaoping Wu

Received 7th August 2014
Accepted 16th September 2014

DOI: 10.1039/c4ra08274e

www.rsc.org/advances

A sensitive sandwich-like electrochemiluminescent (ECL) biosensor was designed for the detection of concanavalin A (ConA) using a C_{60}–reduced graphene oxide (C_{60}–rGO) nanocomposite as a platform and glucose oxidase (GOX) decorated hollow gold nanospheres (HGNSs) as a label. First, C_{60}–rGO with a large surface area was prepared for combining with phenoxy-derivatized dextran, which served as the recognition element for interacting with ConA by biospecific carbohydrate–protein (lectin) interactions. Then, GOX decorated HGNSs (GOX-HGNSs) were linked to the electrode surface through the biospecific interaction between the intrinsic carbohydrate residues of GOX and ConA. These localized GOX and HGNSs amplified the ECL signal of luminol intensely, which was achieved by the efficient catalysis of the GOX towards the oxidation of glucose to *in situ* generate an improved amount of hydrogen peroxide (H_2O_2) as a coreactant, and the excellent catalysis of HGNSs towards the ECL reaction of luminol–H_2O_2. The prepared biosensor exhibited a sensitive response for the determination of ConA, ranging from 0.10 to 100 ng mL^{-1} with a detection limit down to 30 pg mL^{-1} (signal to noise = 3). With excellent stability, sensitivity, selectivity and simplicity, the prepared biosensor showed great prospects in lectin sensing or carbohydrate sensing.

Introduction

Concanavalin A (ConA) is a plant lectin isolated from the jack bean.[1] As a protein, it has an affinity for mannose, glucose and some glycoproteins, such as horseradish peroxidase and glucose oxidase.[2] The investigation of ConA is significant because ConA is a powerful probe to search for cell-surface sugar chains when ConA interacts with the glycoprotein on the cell surface.[3] Besides, ConA affects mitogenic effect and lymphocyte transformation[4] and is applicable to the analysis of malignant tumor cells.[5] Furthermore, ConA was often chosen as a lectin model for further study of carbohydrate–protein interactions.[6–8]

Up to now, the main detection techniques for ConA are electrochemical method including differential pulse voltammetry[9–11] and electrochemical impedance spectroscopy,[12,6] and optic method including fluorescence spectroscopy,[13,14] UV-visible spectroscopy,[15,16] and surface plasmon resonance.[17,18] Generally, these methods suffered from tedious procedures for preparing derivatives of carbohydrate for binding with ConA. What's more, the sensitivity needed to be further improved. These challenges drive us to explore a new detection technique combined with novel signal amplification strategy to realize the highly sensitive determination of ConA.

Electrochemiluminescence is a new detection technique developed in recent years. It has become a powerful analytical tool owing to its advantages such as sensitivity, rapidity, simplicity, controllability, and low background noise.[19] Among various electrochemiluminescent (ECL) systems, luminol–H_2O_2 system integrates inexpensive reagent consumption, low oxidation potential and high emission yields, thus arousing some concern.[20] As well-known, glucose oxidase (GOX) could catalyze the oxidation of glucose to *in situ* generate H_2O_2 which served as a coreactant of luminol to enhance ECL signal of luminol. This amplification strategy will overcome the shortage of instability of H_2O_2 directly as coreactant, improving the sensitivity of the biosensor.[21] Additionally, it is demonstrated that some noble metal nanoparticles especially gold nanoparticles exhibit excellent catalytic performance to directly enhance the ECL signal of luminol–H_2O_2 system.[22] For example, Cui's research group reported ECL biosensors based on luminol functionalized gold nanoparticles for the detection of cardiac troponin I[23] and thrombin[24] with satisfying performance. Since the size and shape would affect the properties of materials,

Education Ministry Key Laboratory on Luminescence and Real-Time Analysis, College of Chemistry and Chemical Engineering, Southwest University, Chongqing 400715, People's Republic of China. E-mail: cshong@swu.edu.cn; Fax: +86-23-68253172; Tel: +86-23-68252277

different nanostructured-gold materials have been synthesized for various applications, such as, nanoparticles,[22–24] nanorods,[25] nanotubes,[26] hollow nanospheres.[27] Among them, hollow gold nanospheres (HGNSs) have attracted considerable interest due to their large surface area, good biocompatibility and excellent conductivity. Particularly, the tunable interior and exterior structure of HGNSs allows more molecules to adsorb on the inside and outside surface of the walls.[28]

Graphene, as a one-atom-thick planar sheet comprising an sp^2-bonded carbon structure, has emerged as a rapidly rising star in the field of nanomaterial science.[29] Fullerene (C_{60}), as a zero-dimensional carbon material, has attracted enormous interest recently owing to its excellent photo/physical behavior, charge transport, and efficient charge separation.[30] The nanocomposite of C_{60} and graphene could combine the merit of C_{60} and graphene, thus showing new properties. For example, this nanocomposite with three-dimensional structure would increase the efficient surface area of graphene. Despite each of them had been applied in several fields, ranging from sensors and photovoltaic cells to nanostructure devices for advanced electronic applications,[29,31] the report about the nanocomposite of C_{60} and graphene is rare. The possible reasons may be as follows. C_{60} is easily soluble in toluene but difficultly soluble in water. However, graphene is usually water-soluble after functionalized by hydrophilic groups such as amido and oxygen containing groups. This difference makes their homogeneous co-interaction difficult. Luckily, the water-soluble C_{60} could be achieved by long-time ultrasonic of the mixture of C_{60}–toluene dispersion and water,[32] which makes the homogeneous co-interaction of C_{60} and graphene possible.

In this work, we synthesized a nanocomposite of C_{60} and reduced graphene oxide (C_{60}–rGO) as matrix for immobilizing biomolecules. Through sandwich scheme, a sensitive ECL biosensor for ConA was designed based on C_{60}–rGO, HGNSs and the advantages of *in situ* generating coreactant. Concretely, using poly(ethylenimine) as linking reagent, C_{60}–rGO was synthesized and cast on the electrode surface for interacting with phenoxy-derivatized dextran (PDN) through π–π stacking. Next, ConA was modified on the electrode surface by biospecific interaction with PDN. Then, the GOX-HGNSs were linked to the electrode surface *via* sandwich biospecific reactions. These localized GOX and HGNSs would greatly amplify the ECL signal of luminol due to the facts that GOX could catalyze the oxidation of glucose to *in situ* generate improved amount of H_2O_2 as coreactant and HGNSs could enhance the ECL signal of luminol–H_2O_2 system. Therefore, as the immobilization amount of ConA increased, the amount of GOX-HGNSs increased, and the ECL signal enhanced. This sandwich scheme not only integrated virtues of C_{60}–rGO and HGNSs, but also utilized a novel signal amplification strategy with *in situ* generating coreactant, thus achieving the highly sensitive detection of ConA.

Experimental

Reagents

Glucose oxidase (GOX), bovine serum albumin (BSA, 96–99%), luminol (5-amino-2, 3-dihydro-1,4-phthalazinedione), concanavalin A (ConA, from CanaValia ensiformis jack bean), 1,2-epoxy-3-phenoxypropane, and phytohaemagglutinin were purchased from Sigma Chemical Co. (St. Louis, MO, USA). Hydrogen tetrachloroaurate ($HAuCl_4 \cdot 4H_2O$) was obtained from Shanghai Chemical Reagent Co., (Shanghai, China). Alpha fetoprotein and carbohydrate antigen 15-3 were received from Biocell Co. (Zhengzhou, China). Poly(ethylenimine) (PEI, 50%) was purchased from Fluka (Switzerland). Graphene oxide (GO) was purchased from Nanking Xianfeng Nano Co. (Nanking, China). Phosphate-buffered saline (PBS) solutions containing 0.10 M KCl, 0.10 mM Ca^{2+} and 0.10 mM Mg^{2+} were prepared with 0.10 M H_3PO_4, adjusted pH with concentrated NaOH solution. Ferricyanide solutions containing 5.0 mM $K_3Fe(CN)_6$ and 5.0 mM $K_4Fe(CN)_6$ were used as a redox reporter. A stock ConA solution (1.0 mg mL^{-1}) was prepared in PBS (0.075 M, pH 7.4) containing 0.10 mM Ca^{2+} and 0.10 mM Mg^{2+} then stored at 4 °C. Herein, Ca^{2+} and Mn^{2+} were necessary to activate ConA conformation.[6] A stock solution of luminol (0.010 M) was prepared by dissolving luminol in 0.10 M NaOH solution and was kept at 4 °C when not in use. Phenoxy-derivatized dextran (PDN) was synthesized according to a previous method in ref. 33, and its molecule structure is shown in Scheme 1, inset (B). All other chemicals were of analytical grade and were used as received. Deionized water was used throughout this study.

Apparatus

Cyclic voltammetry (CV) was performed with a CHI 600D electrochemical work station (Shanghai CH Instruments Co., China). ECL emission was measured using a model MPI-A electrochemiluminescence analyzer (Xi'an Remax Electronic Science & Technology Co. Ltd., China), equipped with a photomultiplier tube with its voltage set at 800 V. The potential was set from 0.2 to 0.8 V at a scan rate of 0.3 V s^{-1} in the detection process. The conventional three-electrode system with a modified glassy carbon electrode (GCE) as working electrode, a saturated calomel electrode (SCE) or Ag/AgCl (saturated KCl) as reference electrode, and a platinum wire as counter electrode

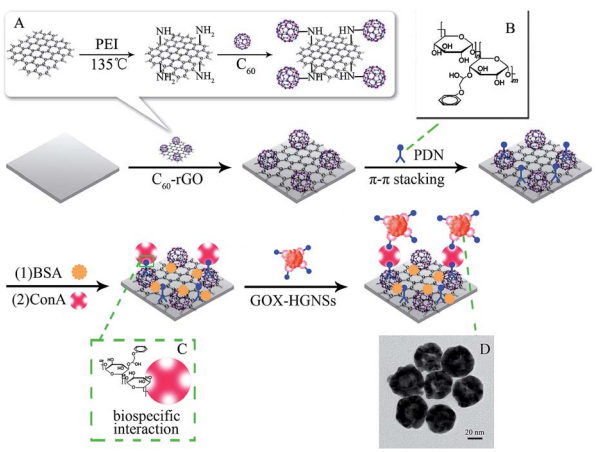

Scheme 1 The schematic representation of the stepwise fabrication process of the biosensor. Inset (A) is the synthesis process of C_{60}–rGO. Inset (B) is the structure of PDN. Inset (C) represents the biospecific interaction. Inset (D) is the TEM image of HGNSs.

was used in the detection process. Absorption spectra were recorded by a UV-2450 UV-vis spectrophotometer from Shimadzu Corp. (Japan). The morphologies of HGNSs were analyzed by scanning electron microscopy (SEM, Hitachi, S-4800, Japan) and transmission electron microscope (TEM, TECNAI 10, Philips Fei Co., Hillsboro, OR). The topographs of different modified films were investigated with atomic force microscopy (AFM, dimension ICON, USA). The fourier-transform infrared spectroscopy (FT-IR) was recorded on a Nexus 670 FT-IR spectrophotometer (Nicolet Instruments) using a KBr pellets. All of the above experiments were carried out at room temperature.

HGNSs preparation

HGNSs were prepared according to the ref. 27 with minor modification. Firstly, 200 μL 0.10 M sodium citrate solution was added into 50 mL double distilled water with rapid magnetic stirring under the nitrogen (N_2) atmosphere. Then, 200 μL of a freshly prepared $NaBH_4$ (1.0 M) and 50 μL $CoCl_2$ (0.50 M) solution were added, respectively. When the color of the solution changed to gray, 150 μL 1% $HAuCl_4$ solution was dropwisely added for six times, each time 25 μL. The color of the solution changed from dark brown to deep blue and then reacted for 30 min under rapid stirring. The resultant mixture was separated and washed by centrifugation with double distilled water to get HGNSs.

Preparation of C_{60}–rGO nanocomposite

First, amido functionalized reduced graphene oxide (rGO) was prepared according to a previously described method.[34] 5.0 mL dispersion of GO sheets (1.0 mg mL^{-1}) and 0.50 mL PEI (3%) were mixed and heated under reflux in an oil bath at 135 °C for about 3 h. The resultant PEI–rGO composite was centrifuged and washed using double distilled water to remove redundant PEI, and then redispersed in 2.0 mL water. Second, water-soluble C_{60} was prepared by adding 5.0 mL 1 mg L^{-1} C_{60}–toluene solution to 5.0 mL ultrapure water. With the aid of ultrasonic agitation, toluene in the solution would completely volatilize, and C_{60} would be transferred to water phase. Afterwards, the yellow product was collected through centrifugation and washed three times with distilled water. Finally, resultant water-soluble C_{60} was mixed with PEI–rGO dispersion, and then keep stirring at room temperature over a night. C_{60} will interact with rGO by the amido on the surface of PEI–rGO to form C_{60}–rGO nanocomposite.[30] After centrifuged to remove the unadsorbed C_{60}, the C_{60}–rGO nanocomposite was obtained and characterized by UV-vis absorption spectrum and FT-IR. The synthesis process of C_{60}–rGO is illustrated in Scheme 1, inset (A).

Fabrication of the ECL biosensor

The glassy carbon electrode (GCE, Φ = 4 mm) was carefully polished with 0.3 μm and 0.05 μm alumina to obtain mirror-like surface, and then ultrasonically washed with ethanol and water, respectively. Subsequently, 8 μL dispersion of C_{60}–rGO was cast on the pretreated GCE and allowed to dry in air. Next, the electrode was immersed into PDN solution. Afterwards, 20 μL of 0.5% BSA solutions was cast onto the electrode for 30 min to block the non-specific binding sites. Then, the resultant electrode was immersed into ConA solution for 1 h to achieve the immobilization of ConA on the electrode surface through the biospecific interaction between ConA and the sugar chains of PDN, as shown in Scheme 1, inset (C). Finally, GOX-HGNSs were linked onto the modified electrode. The modified electrode was cleaned with PBS (pH 7.4) to remove the unstably adsorbed species after every modification step. The schematic diagram of the fabrication of the biosensor is depicted in Scheme 1.

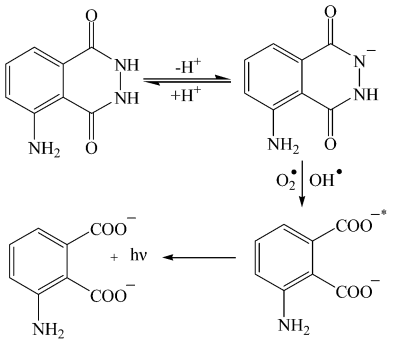

Scheme 2 The mechanism of lumimol ECL emission.

Mechanism of the ECL emission and detection principle of the biosensor

According to the report, the oxidation of luminol is believed to involve the oxygen-related radicals (for example, $OH^{\bullet}$, $O_2^{\bullet -}$, and other radical derivatives) which were generated from H_2O_2 in luminol–H_2O_2 system.[35–38] These active oxygen-related radicals react with luminol monoanion that is from the deprotonation of luminol to produce 3-aminophthalate anions which emit light, as shown in Scheme 2. In the present study, H_2O_2 is generated from the oxidation of glucose catalyzed by GOX. In the presence of enough amount of glucose in detection cell, the concentration of H_2O_2 increases with the amount of GOX. Therefore, the more target ConA are immobilized, the more GOX is assembled through biospecific interaction, and the stronger ECL signal is generated. The intensity of the ECL signal is directly proportional to the concentration of ConA. So ConA can be detected quantitatively using the prepared biosensor.

Results and discussion

Characterization of C_{60}–rGO nanocomposite

Fig. 1(A) shows the UV-vis absorption spectra of rGO, C_{60} and C_{60}–rGO nanocomposite. For C_{60} aqueous solution (curve (a)), three strong optical absorption peaks belonged to the dipole-allowed transitions in pristine C_{60} were observed at 211, 264, and 341 nm, respectively. In the spectrum of rGO (curve (b)), the peak at 265 nm was ascribed to the $\pi \rightarrow \pi^*$ transition of C=C. Curve (c) is the spectrum of C_{60}–rGO nanocomposite. As observed, the three strong optical absorption peaks of C_{60} red-

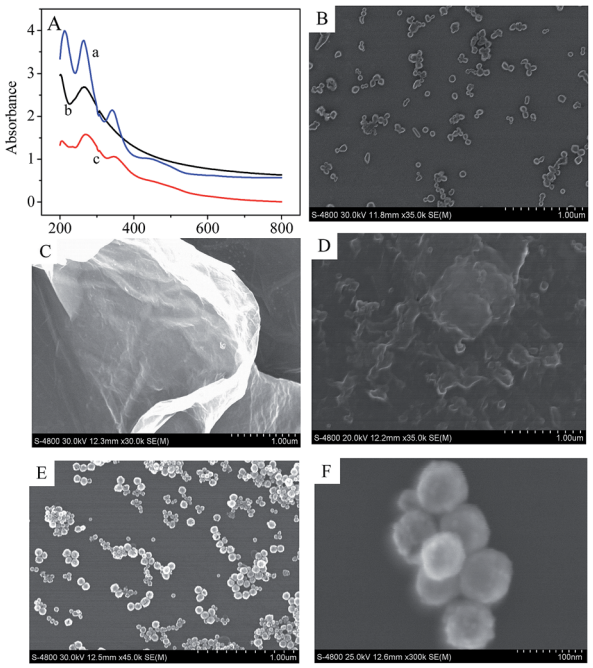

Fig. 1 (A) The UV-vis absorption spectra of (a) C_{60}, (b) rGO, and (c) C_{60}–rGO nanocomposite. SEM images of (B) C_{60}, (C) rGO, (D) C_{60}–rGO, and (E) HGNSs. (F) is an enlarged SEM image of HGNSs.

shifted to 222, 268, 345 nm, respectively, indicating that C_{60} interacted with rGO.

The surface morphologies of rGO, C_{60} and C_{60}–rGO nanocomposite were investigated using SEM. Compared with the SEM image of sole C_{60} (Fig. 1(B)) or rGO (Fig. 1(C)), the SEM image of C_{60}–rGO (Fig. 1(D)) showed many heaves or sunkens, indicating that C_{60}–rGO possessed a larger surface area than C_{60} or rGO for achieving higher biomolecules loading. Fig. 1(E) and (F) display the SEM images of HGNSs. As seen from the enlarged SEM image of HGNSs (Fig. 1(F)), a relatively rough surface morphology was clearly noticed, indicating a large surface area of HGNSs. Also, a darker centre was noticed, which may be attributed to the non-conductivity of hollow structure. The configuration of HGNSs was further confirmed by TEM characterization and the TEM image is shown in Scheme 1, inset (D). As seen from SEM and TEM images of HGNSs, some very small gold particles were observed on the surface of HGNSs. They are maybe the byproduct of the shell growth, namely, some small particles that do not grow into the shell, but break off early in the process.[27,39]

Characterization of the fabrication process of the biosensor

The change in functional groups involved in each reaction step was confirmed by FT-IR technique since it is considered as an important tool for characterizing functional groups. There are four characteristic bands at 524, 573, 1179 and 1425 cm^{-1} (Fig. 2(A) (curve (a))), which consistently matched the typical four dipole-allowed of C_{60}. The PEI reduced graphene oxide showed characteristic peaks at about 1631 cm^{-1} and 1558 cm^{-1}, which were ascribed to the bending vibration of N–H band (Fig. 2(A) (curve (b))). For the FT-IR spectroscopy of C_{60}–rGO (Fig. 2(A) (curve (c))), the peak at 1558 cm^{-1} disappeared and the peak at 1631 cm^{-1} decreased, conforming the fact that C_{60} interacted with rGO *via* amido[30] to successfully achieve C_{60}–rGO nanocomposite. After C_{60}–rGO interacted with PDN, compared with the spectrum of C_{60}–rGO (Fig. 2(A) (curve (c))), a new peak was observed at 1046 cm^{-1} which was attributed to the stretching vibration of C–O–C in dextran (Fig. 2(A) (curve (d))). With the further modification of BSA, ConA and GOX-HGNSs, the bending vibration of N–H band in amino acid residues of proteins at 1640 cm^{-1} and 1550 cm^{-1} appeared again at the spectrum of GOX-HGNSs/ConA/BSA/PDN/C_{60}–rGO composite (Fig. 2(A) (curve (e))). Above results confirmed the change in functional groups involved in each reaction step and showed the successful preparation of the biosensor.

Cyclic voltammetry (CV) is a useful tool to evaluate the assembly process of the modified electrodes. The cyclic voltammograms (CVs) of different modified electrodes using $Fe(CN)_6^{4-/3-}$ as an electroactive probe are presented in Fig. 2(B). As seen from Fig. 2(B), a couple of quasi-reversible redox peaks of the probe was observed at the bare electrode (curve (a)). When the electrode was modified with C_{60}–rGO, an increase in the peak current was observed (curve (b)) owing to that C_{60}–rGO could accelerate the electron transfer rate between the electrode and $Fe(CN)_6^{4-/3-}$, and meanwhile increase the interface area. After consecutively modified with PDN (curve (c)), BSA (curve

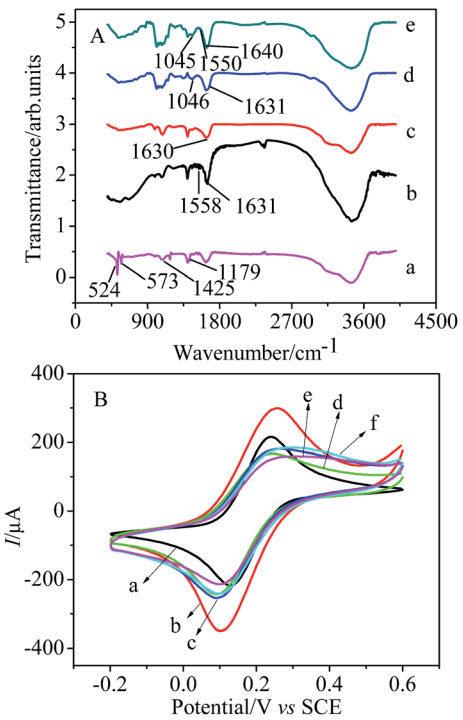

Fig. 2 (A) The FT-IR spectra of (a) C_{60}, (b) rGO, (c) C_{60}–rGO, (d) C_{60}–rGO/PDN, and (e) C_{60}–rGO/PDN/BSA/ConA/GOX-HGNSs. (B) CVs of (a) bare GCE, (b) C_{60}–rGO/GCE, (c) PDN/C_{60}–rGO/GCE, (d) BSA/PDN/C_{60}–rGO/GCE, (e) ConA/BSA/PDN/C_{60}–rGO/GCE, and (f) GOX-HGNSs/ConA/BSA/PDN/C_{60}–rGO/GCE in 5.0 mM $K_3[Fe(CN)_6]$/$K_4[Fe(CN)_6]$ (1 : 1). Scan rate: 50 mV s^{-1}.

(d)), and ConA (curve (e)), the current response successively declined, which was caused by their non-conductivity. When the electrode was incubated in the dispersion of GOX decorated HGNSs (curve (f)), an obvious increase in peak currents was noticed at corresponding CVs, which was ascribed to good conductivity of HGNSs. The CV studies proved that the biosensor has been successfully prepared.

The surface topographies of differently modified films were noticed with AFM and the results are shown in Fig. 3. In Fig. 3(A), a large quantity of C_{60} nanoparticles were homogenously distributed on the rGO nanosheets. After modified with PDN, the surfaces became blurry, which may be attributed to PDN coating on the C_{60}–rGO surface by π–π stacking, seen from Fig. 3(B). When blocked by BSA and further interacted with ConA protein by biospecific interaction (Fig. 3(C)), the AFM image of the resulting film exhibited a smoothing effect as compared with that of C_{60}–rGO/PDN film, which might be due to BSA and ConA molecules filling the interstitial places between C_{60} nanoparticles, suggesting that the ConA and BSA were successively immobilized. After GOX labelled HGNSs were assembled by biospecific interaction between ConA and GOX, some obvious nanoparticles emerged again, suggesting GOX-HGNSs were successfully modified (Fig. 3(D)).

Optimization of analytical conditions

In order to achieve the maximum sensitivity for ConA, experimental parameters including pH and glucose concentration which affect the performance of the biosensor had been discussed.

The pH affects the luminol's ECL signal for the following reasons. (1) Luminol emitted strong chemiluminescent/ECL signal in alkaline condition. (2) The catalytic activity of GOX was affected by pH condition. (3) At low pH, ConA released the metal ions, and consequentially presented in an inactive form, which

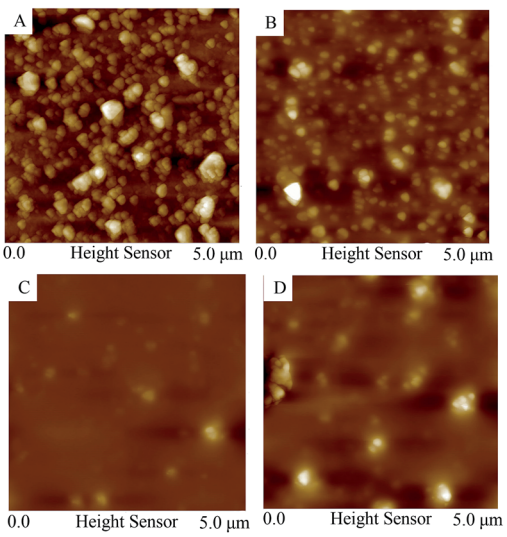

Fig. 3 AFM images of differently modified films: (A) C_{60}–rGO, (B) PDN/C_{60}–rGO, (C) ConA/BSA/PDN/C_{60}–rGO, and (D) GOX-HGNSs/ConA/BSA/PDN/C_{60}–rGO.

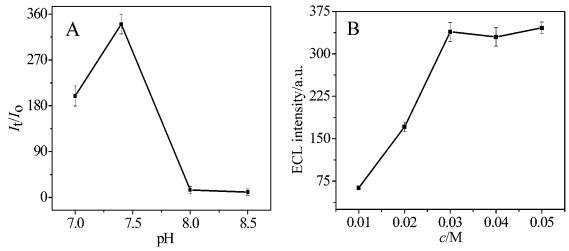

Fig. 4 The effects of (A) pH and (B) glucose concentrations on the ECL response of the biosensor.

prohibited forming effective sandwich configuration, thus leading to a significant decrease in ECL response. Whereas, high pH led to the denaturation of ConA. At room temperature, the ECL signals were recorded at the prepared biosensor (GOX-HGNSs/ConA/BSA/PDN/C_{60}–rGO/GCE) in an ECL detector cell containing different pH PBS with 2.0×10^{-4} M luminol and 0.030 M glucose. The intensity of ECL signal at the biosensor incubated without and with 10 ng mL^{-1} ConA was denoted as I_o and I_t, respectively. I_t/I_o was defined as the standard of optimal value. The corresponding results are shown in Fig. 4(A). As seen, pH 7.4 is optimal for further experiments.

The concentration of glucose needs to be investigated since glucose, as the substrate of enzyme catalytic reaction, could be oxidized to gluconic acid and meanwhile produce H_2O_2, the coreactant of luminol for enhancing ECL signal. The effect of glucose concentration on ECL response was investigated in 0.075 M PBS (pH 7.4) containing 2.0×10^{-4} M luminol at the biosensor incubated with 10 ng mL^{-1} ConA, and the corresponding results are shown in Fig. 4(B). As seen, a strong signal was obtained with 0.030 M glucose. Thus, 0.030 M was chosen in the further experiments.

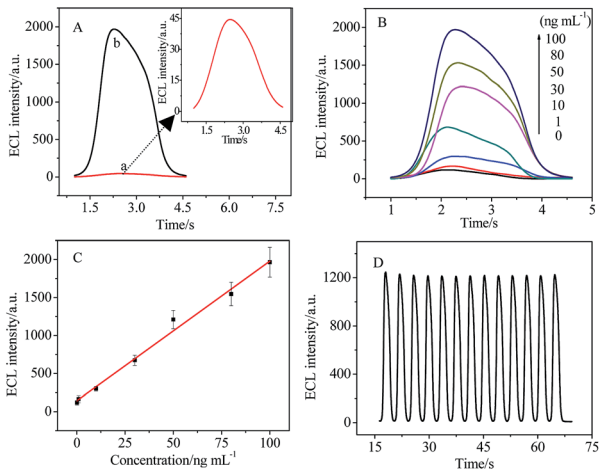

Fig. 5 (A) The ECL response of (a) GOX-HGNSs/BSA/PDN/C_{60}–rGO/GCE and (b) GOX-HGNSs/ConA/BSA/PDN/C_{60}–rGO/GCE. (B) ECL responses of the biosensor to different concentrations of ConA. (C) Calibration curve for ConA assay. (D) The stability of the biosensor incubated with 50 ng mL^{-1} ConA under consecutive cyclic potential scans for 13 cycles. All working buffers were 0.10 M PBS (pH 7.4) containing 2.0×10^{-4} M luminol and 0.030 M glucose.

Table 1 Analytical performance of different detection approaches for the determination of ConA

Immobilization method	Detection approach	Linear range (μg mL^{-1})	Detection limit (μg mL^{-1})	Reference
AuNp/SPCE/Sugar-MPS/ConA	Electrochemical impedance spectroscopy	2.23–40	0.8	6
Glucose assembled onto multi-wall carbon nanotube-polyaniline	Differential pulse voltammetry	0.00034–0.95	0.00010	11
Capture ConA with glycosylated aniline polymer	Electrochemical impedance spectroscopy	0.3–0.15	0.012	12
Trityl-derivatized mannose immobilized on a polystyrene microplate	Fluorescence	0–30	0.12	13
Glycolipid molecules self-assembled onto gold nanoparticles	UV-vis spectrum	2.5–7.5	0.01	15
GO/DexP/ConA/Dex-AuNPs modified gold chips	Surface plasmon resonance	1.0–20.0	0.39	18
GOX-HGNSs/ConA/BSA/PDN/C_{60}–rGO/GCE	Electrochemiluminescence	0.00010–0.10	0.000030	This work

Quantitative analysis of ConA

Fig. 5(A) compared the ECL response of GOX-HGNSs/BSA/PDN/C_{60}–rGO/GCE and GOX-HGNSs/ConA/BSA/PDN/C_{60}–rGO/GCE. Compared with the control electrode GOX-HGNSs/BSA/PDN/C_{60}–rGO/GCE without ConA (curve (a)), the prepared biosensor GOX-HGNSs/ConA/BSA/PDN/C_{60}–rGO/GCE with ConA presented a greatly enhanced ECL signal (curve (b)). This is due to the localized GOX and HGNSs which amplified the luminol ECL signal. The quantitative analysis of ConA was performed at GOX-HGNSs/ConA/BSA/PDN/C_{60}–rGO/GCE under optimal experimental conditions and the results are shown in Fig. 5(B). As seen, with an increase in the incubated ConA concentration, an increase in ECL signal was noticed. The calibration curve (Fig. 5(C)) of ECL intensity *versus* ConA concentration was linear from 0.10 to 100 ng mL^{-1}, with a low detection limit of 30 pg mL^{-1} (signal to noise ratio = 3). The regression equation was I (a.u.) = 18.0c (ng mL^{-1}) + 144.7 (where I was the ECL intensity and c was the concentration of ConA) with a correlation coefficient of 0.994. The details of a comparison between our method and previous methods are provided in Table 1. Compared to the results of most previous reports, our prepared biosensor exhibited a high sensitivity and a low detection limit, which was due to the following reasons. First, the C_{60}–rGO as the supporting nanomaterials enabled low background ECL signal. Second, through a sandwich protocol, the localized GOX and HGNSs were assembled onto the electrode which could generate coreactant *in situ* for ECL signal enhancement.

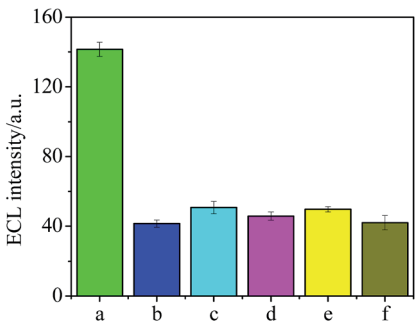

Fig. 6 The ECL response at the biosensor for (a) 1 ng mL^{-1} ConA, (b) blank solution, (c) carbohydrate antigen 15-3, (d) phytohaemagglutinin, (e) alpha fetoprotein, and (f) BSA.

Reproducibility, stability, and selectivity of ECL biosensor

The reproducibility of the biosensor was estimated by testing the 1 ng mL^{-1} ConA with five modified electrodes in the same batch. The relative standard deviation (RSD) was found to be 4.6%, indicating an acceptable reproducibility.

The stability of the biosensor was investigated by testing its ECL response in PBS under consecutive cyclic potential scans for 13 cycles. The curve of ECL signal (*vs.* time) is shown in Fig. 5(D) (RSD = 1.0%).

To further study the selectivity of the biosensor, different interfering agents such as alpha fetoprotein (50 ng mL^{-1}), BSA (0.5%, w/w), carbohydrate antigen 15-3 (0.1 U mL^{-1}) and phytohaemagglutinin (100 ng mL^{-1}) were investigated. The corresponding results are shown in Fig. 6. As seen, the change in ECL signal caused by these interfering substances was neglectable compared with that of blank solution. However, the ECL signal obviously enhanced for 1 ng mL^{-1} ConA compared with the blank solution. This result indicated a good selectivity of the prepared biosensor towards ConA.

Conclusions

In summary, a novel sandwich ECL biosensor for the sensitive detection of ConA was developed using C_{60}–rGO as a substrate for the immobilization of PDN and GOX-HGNSs as amplification reagent. The amplification of the luminol ECL signal was achieved as follows. (1) HGNSs own large surface area, and good biocompatibility, which is propitious to immobilize more GOX for efficient catalysis towards glucose to *in situ* generate H_2O_2. (2) Due to excellent conductivity and large surface area, and excellent electroactivity to luminol oxidization, the HGNSs could amplify the ECL signal of luminol. Additionally, C_{60}–rGO with large surface area as a substrate for immobilizing PDN presented low background signal. Therefore, the prepared biosensor presented high sensitivity towards the determination

of ConA. Furthermore, a satisfying stability, selectivity and simplicity were obtained. This scheme might show a great prospect in lectin sensing or carbohydrate sensing and provide an efficient and promising platform for the fabrication of bioelectrochemical devices.

Acknowledgements

This work was financially supported by the NNSF of China (21075100, 21275119, 21105081), Ministry of Education of China (Project 708073), Research Fund for the Doctoral Program of Higher Education (RFDP) (20110182120010), Natural Science Foundation of Chongqing City (CSTC-2011BA7003, CSTC-2014JCYJA20005), and the Fundamental Research Funds for the Central Universities (XDJK2013A008, XDJK2013A27), China.

Notes and references

1 R. J. Russell and M. V. Pishko, *Anal. Chem.*, 1999, **71**, 3126.
2 W. J. Li, R. Yuan and Y. Q. Chai, *J. Phys. Chem. C*, 2010, **114**, 21397.
3 T. Horlacher and P. H. Seeberger, *Chem. Soc. Rev.*, 2008, **37**, 1414.
4 L. Shou, S. A. Schwartz and R. A. Good, *J. Exp. Med.*, 1976, **143**, 1100.
5 A. Kobata and J. Amano, *Immunol. Cell Biol.*, 2005, **83**, 429.
6 O. A. Loaiza, P. J. Lamas-Ardisana, E. Jubete, E. Ochoteco, I. Loinaz, G. Cabanero, I. García and S. Penadés, *Anal. Chem.*, 2011, **83**, 2987.
7 G. Bellapadrona, A. B. Tesler, D. Grünstein, L. H. Hossain, R. Kikkeri, P. H. Seeberger, A. Vaskevich and I. Rubinstein, *Anal. Chem.*, 2012, **84**, 232.
8 C. F. Huang, G. H. Yao, R. P. Liang and J. D. Qiu, *Biosens. Bioelectron.*, 2013, **50**, 305.
9 K. Sugawara, T. Kadoya and H. Kuramitz, *Anal. Chim. Acta*, 2014, **814**, 55.
10 C. X. Guo, P. Boullanger, L. Jiang and T. Liu, *Colloids Surf., B*, 2008, **62**, 146.
11 F. X. Hu, S. H. Chen, C. Y. Wang, R. Yuan, Y. Xiang and C. Wang, *Biosens. Bioelectron.*, 2012, **34**, 202.
12 Z. Wang, C. Y. Sun, G. Vegesna, H. Y. Liu, Y. Liu, J. H. Li and X. Q. Zeng, *Biosens. Bioelectron.*, 2013, **46**, 183.
13 C. C. Huang, C. T. Chen, Y. C. Shiang, Z. H. Lin and H. T. Chang, *Anal. Chem.*, 2009, **81**, 875.
14 L. Zou, H. L. Pang, P. H. Chan, Z. S. Huang, L. Q. Gu and K. Y. Wong, *Carbohydr. Res.*, 2008, **343**, 2932.
15 C. X. Guo, P. Boullanger, L. Jiang and T. Liu, *Biosens. Bioelectron.*, 2007, **22**, 1830.
16 D. C. Hone, A. H. Haines and D. A. Russell, *Langmuir*, 2003, **19**, 7141.
17 S. Morokoshi, K. Ohhori, K. Mizukami and H. Kitano, *Langmuir*, 2004, **20**, 8897.
18 C. F. Huang, G. H. Yao, R. P. Liang and J. D. Qiu, *Biosens. Bioelectron.*, 2013, **50**, 305.
19 W. J. Miao, *Chem. Rev.*, 2008, **108**, 2506.
20 L. Z. Hu and G. B. Xu, *Chem. Soc. Rev.*, 2010, **39**, 3275.
21 Y. L. Cao, R. Yuan, Y. Q. Chai, L. Mao, H. Niu, H. J. Liu and Y. Zhuo, *Biosens. Bioelectron.*, 2012, **31**, 305.
22 S. J. Xu, Y. Liu, T. H. Wang and J. H. Li, *Anal. Chem.*, 2010, **82**, 9566.
23 F. Li, Y. Q. Yu and H. Cui, *Analyst*, 2013, **138**, 1844.
24 F. Li and H. Cui, *Biosens. Bioelectron.*, 2013, **39**, 261.
25 Z. Zhang and M. S. Lin, *RSC Adv.*, 2014, **4**, 17760.
26 D. C. Rodrigues, G. F. S. Andrade and M. L. A. Temperini, *Phys. Chem. Chem. Phys.*, 2013, **15**, 1169.
27 A. M. Schwartzberg, T. Y. Oshiro, J. Z. Zhang, T. Huser and C. E. Talley, *Anal. Chem.*, 2006, **78**, 4732.
28 V. G. Rao, C. Banerjee, S. Mandal, S. Ghosh and N. Sarkar, *RSC Adv.*, 2013, **3**, 14963.
29 D. Chen, H. B. Feng and J. H. Li, *Chem. Rev.*, 2012, **112**, 6027.
30 H. Wu, S. H. Fan, X. Y. Jin, H. Zhang, H. Chen, Z. Dai and X. Y. Zou, *Anal. Chem.*, 2014, **86**, 6285.
31 X. Zhong, R. Yuan and Y. Q. Chai, *Chem. Commun.*, 2012, **48**, 597.
32 P. F. Wei, L. Zhang, Y. Lu, N. Man and L. P. Wen, *Nanotechnology*, 2010, **21**, 495101.
33 J. Huang, L. Zhang, R. P. Liang and J. D. Qiu, *Biosens. Bioelectron.*, 2013, **41**, 430.
34 L. Y. Cao, Y. L. Liu, B. H. Zhang and L. H. Lu, *ACS Appl. Mater. Interfaces*, 2010, **2**, 2339.
35 G. Mereĭnyi and S. L. Johan, *J. Am. Chem. Soc.*, 1980, **102**, 5830.
36 A. N. Diaz and J. A. Garcia, *Anal. Chem.*, 1994, **66**, 988.
37 R. Joseph and O. N. Sigurd, *J. Phys. Chem.*, 1969, **73**, 3736.
38 S. F. Li, X. M. Zhang, W. X. Du, Y. H. Ni and X. W. Wei, *J. Phys. Chem. C*, 2009, **113**, 1046.
39 A. M. Schwartzberg, T. Y. Olson, C. E. Talley and J. Z. Zhang, *J. Phys. Chem. B*, 2006, **110**, 19935.